Available online at www.sciencedirect.com

SCIENCE DIRECT®

International Journal of Mass Spectrometry 230 (2003) 25–31

www.elsevier.com/locate/ijms

Characteristics of cylindrical ion trap

Won-Wook Lee[a,b,1], Cha-Hwan Oh[a,b,*], Pill-Soo Kim[a], Mo Yang[c], Kyuseok Song[d]

[a] *Department of Physics, Hanyang University, Seoul 133-791, South Korea*
[b] *Quantum Photonic Science Research Center, Seoul 133-791, South Korea*
[c] *Samyang Chemical Co. Ltd., Seoul 137-073, South Korea*
[d] *Laboratory for Quantum Optics, Korea Atomic Energy Research Institute, Taejon 305-600, South Korea*

Received 21 January 2003; received in revised form 2 July 2003; accepted 5 August 2003

Abstract

The characteristics of cylindrical ion trap (CIT) for a miniaturized mass spectrometer was investigated. The equation of motion for an ion was derived, and the stability region in the CIT was calculated and compared with that in the Paul trap. As the result, the geometric relation between the CIT and the Paul trap was obtained analytically, which is useful to easily analyze the stability of ion motion in the CIT. Through the pseudo-potential approach, the stability space in the CIT was discussed qualitatively. The stability space which indicated the stability of ion motion in space was quantitatively calculated by the equation of motion and analyzed. It was reconfirmed that the stability space was dependent on the position of ion, differently from the Paul trap.

Keywords: Cylindrical ion trap; Mass spectrometer; Equation of motion; Ion stability

1. Introduction

Quadrupole ion trap invented by Paul and Steinwedel [1] has been widely applied to mass spectrometry [2,3], ion cooling and spectroscopy [4–6], frequency standards [7,8], quantum computing [9,10], and so on.

Ion trap mass spectrometer has developed through several stages to their current stage of relatively high performance and increasing popularity [2,3]. To apply to various objectives, various geometries of ion trap for the mass spectrometer have been suggested [11]. Specially, the cylindrical ion trap (CIT) has received much attention of a number of research groups because of several merits. The CIT is easier to fabricate than the Paul trap which has hyperbolic surfaces [12–14]. And the relative simplicity and small size of the CIT make it an ideal candidate for miniaturization. With these interests, many groups in, such as Purdue University [15,16] and Oak Ridge National Laboratory [17,18] have researched on the applications of the CIT to a miniaturized mass spectrometer.

The CIT has a simple geometry, but the equation of motion is complicate and difficult to solve analytically. Berilan and Audoin [12] suggested the equation of motion and described the potential distribution in the CIT. Bonner et al. [13] also suggested the potential distribution in the CIT expressed with modified Bessel functions and triangular functions.

The Paul trap has hyperbolic surfaces, but the equation of motion is given by the Mathieu equation which solution is well known. Therefore, it is very useful for the analysis of the ion motion in the CIT to know the geometric relation between the CIT and the Paul trap which gives the same characteristics for the motion of an ion in the traps.

In this paper, we derived the equations of ion motion in the CIT, and calculated the stability region for the ion motion. Also, the geometric relation between the CIT and the Paul trap was obtained. Using the approaches with pseudo-potential and the equations of ion motion, the spatial stability of ion motion in the CIT was discussed.

2. Equation of motion

The CIT is the ion trap with cylindrical geometry as shown in Fig. 1. The CIT is composed of a ring and two end cap electrodes facing each other in the z-axis. z_1 expresses the

---

[*] Corresponding author.

E-mail addresses: impkissu@hanmail.net (W.-W. Lee), choh@hanyang.ac.kr (C.-H. Oh).

[1] Tel.: 82-222900926; fax: +82-222973812.

1387-3806/$ – see front matter © 2003 Elsevier B.V. All rights reserved.
doi:10.1016/j.ijms.2003.08.001

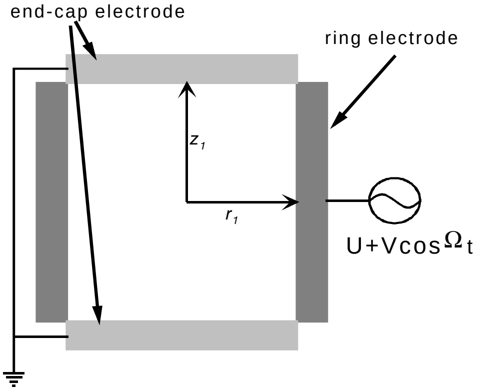

Fig. 1. The cross-sectional view of the CIT in the *r*–*z*-plane.

distance from the center of the CIT to the end cap and r_1 the distance from the center of the CIT to the nearest ring surface. To obtain the equation of motion in the CIT, we selected the potential distribution suggested by Bonner et al. [13];

$$\Phi(r,z)=4\Phi_0\sum_{n=0}^{\infty}\frac{(-1)^n}{(2n+1)\pi}\frac{I_0(rl_n)}{I_0(r_1l_n)}\cos(l_nz),\quad l_n=\frac{(2n+1)\pi}{2z_1}\tag{1}$$

where I_0 is 0th modified Bessel function of the 1st kind. Based on this expression, we derived the equation of motion of an ion in the CIT.

The equation of motion for a singly charged positive ion is given by

$$\frac{\mathrm{d}^2\vec{r}}{\mathrm{d}t^2}=-\frac{e}{m}\nabla\Phi\tag{2}$$

where *m* is the ion mass and *e* is the electronic charge. When both the end-cap electrodes are grounded and an electric potential of $\Phi_0=U+V\cos(\Omega t+\gamma)$ is applied to the ring electrode, Eq. (2) can be written as

$$\frac{\mathrm{d}^2r}{\mathrm{d}t^2}=-\frac{2e}{mz_1}(U+V\cos\Omega t)\sum_{n=0}^{\infty}\frac{I_1(rl_n)}{I_0(r_1l_n)}\cos(n\pi)\cos(l_nz)\tag{3}$$

$$\frac{\mathrm{d}^2z}{\mathrm{d}t^2}=-\frac{2e}{mz_1}(U+V\cos\Omega t)\times\sum_{n=0}^{\infty}\frac{I_0(rl_n)}{I_0(r_1l_n)}\cos((n+1)\pi)\sin(l_nz)\tag{4}$$

where *U* and *V* are dc and rf voltages, respectively. Ω is the angular frequency of the rf voltage with an initial phase angle of γ. In Eqs. (3) and (4), γ was set to zero for simplicity. Defining the parameters for the CIT, such that

$$\tau=\frac{1}{2}\Omega t,\quad \alpha_r=\frac{8eU}{mz_1^2\Omega^2},\quad \xi_r=\frac{-4eU}{mz_1^2\Omega^2},\quad \alpha_z=\frac{-16eV}{mz_1^2\Omega^2},\quad \xi_z=\frac{8eV}{mz_1^2\Omega^2}\tag{5}$$

Eqs. (3) and (4) become

$$\frac{\mathrm{d}^2r}{\mathrm{d}\tau^2}+(\alpha_r-2\xi_r\cos2\tau)R(r,z)=0,\quad \frac{\mathrm{d}^2z}{\mathrm{d}\tau^2}+(\alpha_z-2\xi_z\cos2\tau)Z(r,z)=0,\tag{6}$$

where $R(r, z)$ and $Z(r, z)$ are given by

$$R(r,z)=z_1\sum_{n=0}^{\infty}\frac{I_1(rl_n)}{I_0(r_1l_n)}\cos(n\pi)\cos(zl_n),\quad Z(r,z)=\frac{z_1}{2}\sum_{n=0}^{\infty}\frac{I_0(rl_n)}{I_0(r_1l_n)}\cos(n\pi)\sin(zl_n)\tag{7}$$

To obtain the numerical solution of the Mathieu equation of the Paul trap and equation of ion's motion in the CIT, 4th Runge–Kutta method was used. Since there exists no force in the ideal center of the CIT, the ion's initial position was $r_i=1\times10^{-9}$ m, $z_i=1\times10^{-9}$ m to avoid the ideal center of the CIT. The ion's velocities were zero for the *r*-direction and the *z*-direction. The ion's stability was obtained by calculating the equation of ion's motion with 4th Runge–Kutta method.

Fig. 2 shows the stability regions for the Paul trap and the CIT. The solid lines and the open diamonds are the stability regions for the Paul trap. The solid lines were calculated from the stability condition of the Mathieu equation for the Paul trap [2]. The open diamonds were obtained from the numerical solution of the equation of motion in the Paul trap. As shown in the figure, the open diamonds well matched with the solid lines. From this, we confirmed that

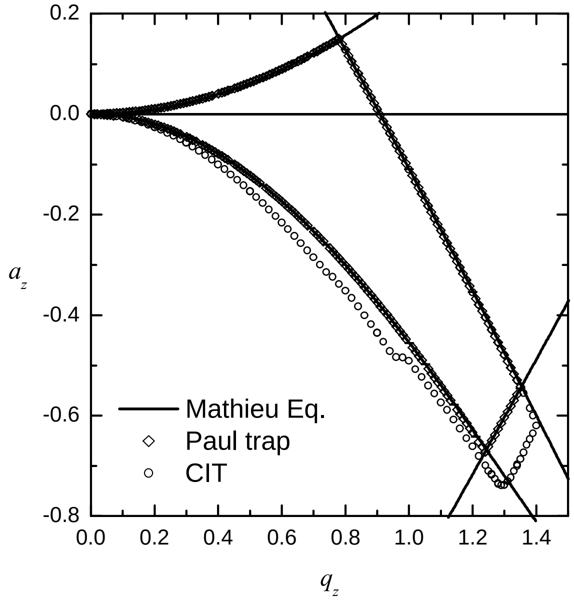

Fig. 2. The stability regions. The solid lines were calculated from the stability condition of the Mathieu equation for the Paul trap, the open diamonds and the open circles were obtained from the numerical solutions of the equation of motion in the Paul trap and the CIT, respectively. The geometry of the CIT was fixed at $r_1 = 2.5$ and $z_1 = 2.88$ mm.

the calculation of the stability region from the numerical solution of the equation of motion in the trap could be successfully applied to the determination of the stability region in the trap. The open circles were calculated from the numerical solution of Eqs. (3) and (4) for the CIT. The stability region of the CIT was very similar to the stability region of the Paul trap. However, the stability region of the CIT was expanded when a_z value increased in negative. In Eqs. (3) and (4), the $R(r, z)$ and $Z(r, z)$ are consisted of modified Bessel functions. And the relation between $R(r, z)$ and $Z(r, z)$ is different from the relation between the r and the z in the Mathieu equation for the Paul trap, which are independent of each other. However, the positions of r and z in the CIT depend on each other, i.e., $R(r, z)$ is not independent of $Z(r, z)$. The high-order effect of modified Bessel function in $R(r, z)$ and $Z(r, z)$ should cause the expansion of stability region in high dc voltage. Even though there was a little difference in the negative a_z region, the stabilities in the z-axis ($a_z = 0$) well matched each other. The mass spectrometer using mass selective instability scan method uses the condition of $a_z = 0$ as the operation line. In that case, the stability along the z-axis in the CIT can be interpreted by the stability condition of the Paul trap. This approach was treated by Benilan and Audoin [12]. They approximated the term in their equation of motion, which corresponds to $R(r, z)$ and $Z(r, z)$ in Eq. (6), to r and z, respectively. Based on this approximation, they proposed the geometric relation between the CIT and the Paul trap. However, the high-order in $R(r, z)$ and $Z(r, z)$ cannot be neglected, and their approximation gives large difference when the high-order terms in $R(r, z)$ and $Z(r, z)$ cannot be negligible. Therefore, we derived the concrete expression for the geometric relation between the Paul trap and the CIT using Eq. (6) in this paper.

3. Geometric relation

At first, to understand the characteristics of equation of motion in the CIT, we took six terms in the series as follows, which was enough since the higher terms were negligible.

$$\begin{aligned}\sum_{n=0}^{\infty}\frac{(-1)^n}{(2n+1)\pi}\frac{I_0(rl_n)}{I_0(r_1l_n)} &\approx \left[\frac{1}{\pi}\frac{I_0(rl_0)}{I_0(r_1l_0)}-\frac{1}{3\pi}\frac{I_0(rl_1)}{I_0(r_1l_1)}\right]\\ &\quad+\left[\frac{1}{5\pi}\frac{I_0(rl_2)}{I_0(r_1l_2)}-\frac{1}{7\pi}\frac{I_0(rl_3)}{I_0(r_1l_3)}\right]\\ &\quad+\left[\frac{1}{9\pi}\frac{I_0(rl_4)}{I_0(r_1l_4)}-\frac{1}{11\pi}\frac{I_0(rl_5)}{I_0(r_1l_5)}\right] \qquad (8)\end{aligned}$$

If we assume $z \ll z_1$, in the center region, $\cos(zl_n)$ and $\sin(zl_n)$ can be approximated by

$$\cos(zl_n) \approx 1-\frac{1}{2!}(zl_n)^2, \quad \sin(zl_n) \approx zl_n-\frac{1}{3!}(zl_n)^3 \qquad (9)$$

respectively. Therefore, Eq. (4) becomes

$$\frac{\mathrm{d}^2z}{\mathrm{d}t^2}-\frac{e\pi}{mz_1^2}\left[\mathbf{A}-\frac{\pi^2}{24}\mathbf{B}\left(\frac{z}{z_1}\right)^2\right](U+V\cos(\Omega t))z=0 \qquad (10)$$

where,

$$\begin{aligned}\mathbf{A} &\equiv \frac{I_0(rl_0)}{I_0(r_1l_0)}-3\frac{I_0(rl_1)}{I_0(r_1l_1)}+5\frac{I_0(rl_2)}{I_0(r_1l_2)}-7\frac{I_0(rl_3)}{I_0(r_1l_3)}\\ &\quad+9\frac{I_0(rl_4)}{I_0(r_1l_4)}-11\frac{I_0(rl_5)}{I_0(r_1l_5)},\\ \mathbf{B} &\equiv \frac{I_0(rl_0)}{I_0(r_1l_0)}-3^3\frac{I_0(rl_1)}{I_0(r_1l_1)}+5^3\frac{I_0(rl_2)}{I_0(r_1l_2)}-7^3\frac{I_0(rl_3)}{I_0(r_1l_3)}\\ &\quad+9^3\frac{I_0(rl_4)}{I_0(r_1l_4)}-11^3\frac{I_0(rl_5)}{I_0(r_1l_5)} \qquad (11)\end{aligned}$$

Again, Eq. (10) can be expressed by

$$\begin{aligned}&\frac{\mathrm{d}^2z}{\mathrm{d}\tau^2}+(\alpha_z\eta-2\xi_z\eta\cos(2\tau))z=0,\\ &\eta=\frac{\pi}{4}\left[\mathbf{A}-\frac{\pi^2}{24}\mathbf{B}\left(\frac{z}{z_1}\right)^2\right] \qquad (12)\end{aligned}$$

When we define trap parameters as follows:

$$a_{z,\mathrm{CIT}}=\alpha_z\eta, \quad q_{z,\mathrm{CIT}}=\xi_z\eta \qquad (13)$$

Eq. (12) becomes

$$\frac{\mathrm{d}^2z}{\mathrm{d}\tau^2}+(a_{z,\mathrm{CIT}}-2q_{z,\mathrm{CIT}}\cos(2\tau))z=0 \qquad (14)$$

Eq. (14) is very similar form to the Mathieu equation for the Paul trap. This equation is applicable in the condition of $z \ll z_1$. When an ion is located far from the center of the CIT, the high-order terms of **B** should be considered. However, ions are trapped near the center of ion trap in most situation. Therefore, $r \approx 0$, then **A** and **B** are nearly constants as can be known in Eq. (11). Because $z \approx 0$, η can be expressed by

$$\eta=\frac{\pi}{4}\mathbf{A} \qquad (15)$$

and η has a constant value. The constant η means that trap parameters of the CIT, $a_{z,\mathrm{CIT}}$ and $q_{z,\mathrm{CIT}}$, are only dependent on dc voltage and rf voltage. Therefore, η gives the unique geometry of the Paul trap corresponding to the CIT. Of course, when the ions are located far from the center of the CIT, η value is not constant and η value changes with the position of ion. However, we confirmed that η value was a constant value in the condition of $z < z_1/10$.

When the η is the constant, Eq. (14) is perfectly same to the Mathieu equation of the Paul trap. From this fact, there exists the relation as follows:

$$q_{z,\mathrm{CIT}}=\xi_z\eta=q_z, \quad r_0=z_1\sqrt{\frac{2}{\pi\mathbf{A}}} \qquad (16)$$

where q_z is the trap parameter of the Paul trap, r_0 is the distance between center of the Paul trap and ring electrode

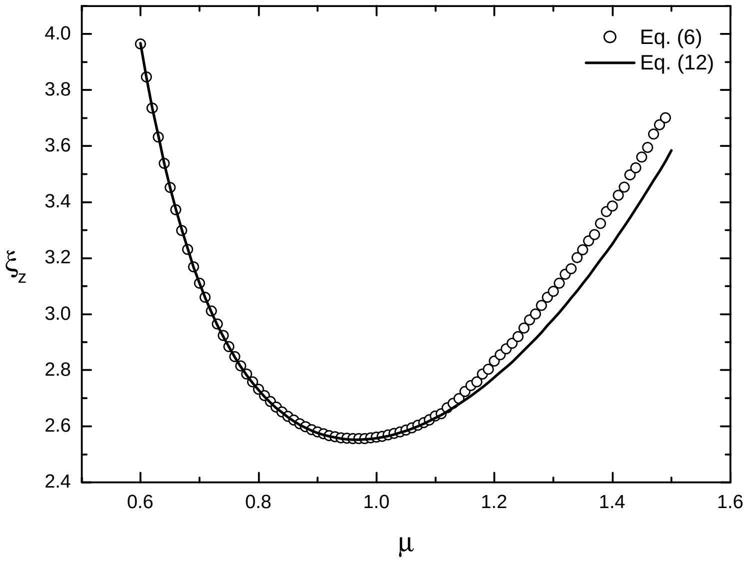

Fig. 3. The comparison of ξ_z obtained by numerical calculation of equation of motion for an ion that by Eq. (12).

and z_1 is the distance between the center of the CIT and an end-cap electrode, respectively. Eq. (16) means that the relation between the geometry of the Paul trap and of the CIT, i.e., Eq. (16) tells us that we can consider the stability in the Paul trap with r_0 given by Eq. (16) if we want to know the stability of ion motion in the CIT with z_1. Also, Eq. (16) can be obtained by potential distribution using Eqs. (8), (9) and (15).

The validity of Eqs. (14) and (16) could be check by ion's instability in Fig. 3. In the Paul trap, if r_0 is known, then the geometry of the Paul trap is uniquely determined. However, even if the z_1 value is fixed, the CIT may have various r_1 values according to the η values in Eq. (12). Therefore, ξ_z in Eq. (13) has different value for each μ ($=r_1/z_1$) value which expresses geometries of the CIT. Fig. 3 shows the ξ_z corresponding to $q_{z,\mathrm{CIT}} = 0.908$. The solid line and open circles express the ξ_z obtained by calculating Eqs. (6) and (14), respectively. The results calculated Eqs. (6) and (14) were perfectly coincided with each other in $\mu < 1.1$. Although the results of Fig. 3 do not coincide well with each other $\mu < 1.1$, the results have a similar tendency, i.e., when the geometry of the CIT is $\mu < 1.1$, the potential distribution and equation of motion of the CIT can treated as those of the Paul trap with the geometric relation given by Eq. (16). Actually, this might be the reason that most reported optimum geometries of the CIT were less than $\mu = 1$, they tried to find the geometry of the CIT corresponding to the Paul trap [15–18]. Therefore, the geometric relation in Eq. (16) can be well applied to actual mass spectrometer.

4. Pseudo-potential

Pseudo-potential is the time-averaged potential applied to an ion in the ion trap. The pseudo-potential of the Paul trap was suggested by Dehmelt [19]. The pseudo-potential of the CIT also could be obtained by the same method. The ion's amplitude z of trajectory in the CIT can be replaced by a sum of two amplitudes, Z, representing the secular motion and δ, the micro motion, as follows:

$$z = Z + \delta \tag{17}$$

With the additional assumptions (i) $\delta \ll Z$ and (ii) $\mathrm{d}\delta/\mathrm{d}\tau \gg \mathrm{d}Z/\mathrm{d}\tau$ Eq. (12) yields

$$\frac{\mathrm{d}^2\delta}{\mathrm{d}\tau^2} = \frac{\pi}{2}\mathbf{A}\xi_z Z\cos(2\tau) - \frac{\pi^3}{48}\mathbf{B}\xi_z\frac{Z^3}{z_1^2}\cos(2\tau) \tag{18}$$

Assuming, further, that $\alpha_z \ll \xi_z$ and Z is constant over a period of high-frequency rf oscillation, Eq. (18) can be integrated to give

$$\delta = -\frac{\pi}{8}\xi_z\rho Z\cos(2\tau) \tag{19}$$

Substituting in Eq. (17) for δ from Eq. (19) we obtain

$$z = Z - \frac{\pi}{8}\xi_z\rho Z\cos(2\tau), \qquad \rho = \mathbf{A} - \frac{\pi^2}{24}\mathbf{B}\frac{Z^2}{z_1^2} \tag{20}$$

where ρ is different from η. ρ consists of the amplitude of secular motion and η consists of that of whole trajectory with secular motion and micro motion. Also, when the z in Eq. (10) is substitute for z from Eq. (20), the average $\mathrm{d}^2Z/\mathrm{d}\tau^2$ can be written as

$$\begin{aligned}\left\langle\frac{\mathrm{d}^2Z}{\mathrm{d}\tau^2}\right\rangle = &-\frac{\pi}{4}\mathbf{A}\alpha_z Z + \frac{\pi^3}{96}\mathbf{B}\alpha_z\left(\frac{Z}{z_1}\right)^2 Z \\ &+ \frac{3\pi^5}{12288}\mathbf{B}\alpha_z\xi_z^2\rho^2\left(\frac{Z}{z_1}\right)^2 Z - \frac{\pi^2}{32}\mathbf{A}\xi_z^2\rho Z \\ &+ \frac{3\pi^4}{768}\mathbf{B}\xi_z^2\rho\left(\frac{Z}{z_1}\right)^2 Z + \frac{3\pi^6}{196608}\mathbf{B}\xi_z^4\rho^3\left(\frac{Z}{z_1}\right)^2 Z\end{aligned} \tag{21}$$

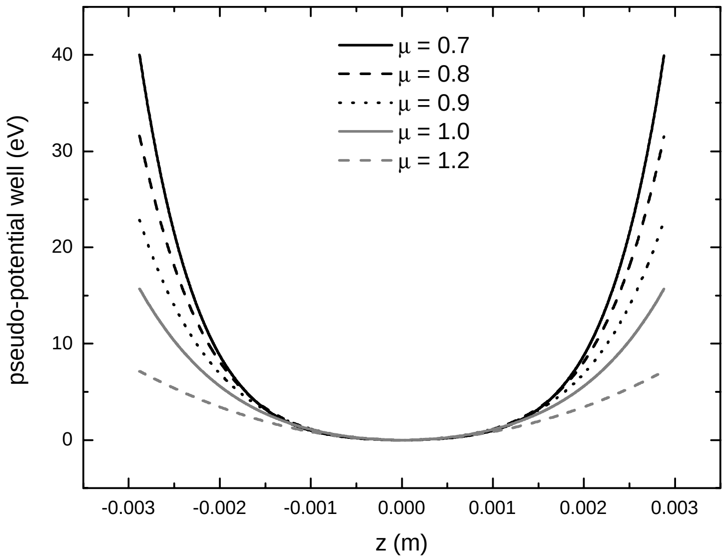

Fig. 4. Pseudo-potential of CIT at $r = 0$. The z_1 and *m/z* were fixed at 2.88 mm and 100 Th, respectively. The rf frequency and rf voltage were fixed at 2 MHz and 150 V, respectively.

Then, the average of the acceleration $\mathrm{d}^2\delta/\mathrm{d}\tau^2$ over a period of rf voltage is zero. For no dc bias condition, that is, $\alpha_z = 0$, we obtain

$$\left\langle \frac{\mathrm{d}^2 Z}{\mathrm{d}t^2} \right\rangle = -\frac{\pi^2}{128}\mathbf{A}\xi_z^2\rho\Omega^2 Z + \frac{\pi^4}{384}\left(\frac{Z}{z}\right)^2\left[\frac{3}{8}\xi_z^2\rho + \frac{3\pi^2}{2048}\xi_z^4\rho^3\right]\mathbf{B}\Omega^2 Z \qquad (22)$$

Following $\mathrm{d}^2 z/\mathrm{d}t^2 = -(e/m)\nabla\Phi$, the average force on an ion of mass m and charge e is

$$m\left\langle \frac{\mathrm{d}^2 Z}{\mathrm{d}t^2} \right\rangle_{1\,\mathrm{rf\,cycle}} = -e\frac{\partial \overline{D_z}}{\partial z} \qquad (23)$$

where $\overline{D_z}$ is the depth of the pseudo-potential well in which ions oscillate in the z-direction. Using Eqs. (22) and (23), the $\overline{D_z}$ can be expressed as

$$\overline{D_z} = \int_{Z=0}^{Z=z} \frac{\partial D_z}{\partial Z}\mathrm{d}Z = \frac{mq_{z,\mathrm{CIT}}^2\Omega^2 z^2}{16e} + \mathbf{H.O.} \qquad (24)$$

$$\mathbf{H.O.} = \left(\frac{m}{e}\right)\frac{\pi^6}{256\cdot 1024}\left[-\frac{1}{4}\mathbf{A}^3\mathbf{B} + \frac{\pi^2}{2\cdot 24}\mathbf{A}^2\mathbf{B}^2\left(\frac{z}{Z_1}\right)^2 - \frac{3\pi^4}{8\cdot 24^2}\mathbf{A}\mathbf{B}^3\left(\frac{z}{Z_1}\right)^4 + \frac{\pi^6}{10\cdot 24^3}\mathbf{B}^4\left(\frac{z}{Z_1}\right)^6\right] \times \xi_z^4\Omega^2\left(\frac{z}{Z_1}\right)^2 z^2 \qquad (25)$$

When a time-varying rf voltage was applied to CIT, Eq. (24) provided the pseudo-potential of CIT. The pseudo-potential of CIT consisted of two terms; the one was the same to the pseudo-potential of Paul trap and the other was the high-order terms in Eq. (25). The high-order terms were negligible since the value of **H.O.** in Eq. (24) had a difference less than 2% compared with no **H.O.** That is to say, Eq. (24) could be approximated to

$$\overline{D_z} = \frac{mq_{z,\mathrm{CIT}}^2\Omega^2 z^2}{16e} \qquad (26)$$

where $q_{z,\mathrm{CIT}}$ was already defined in Eq. (13). When η is constant, Eq. (14) is the perfectly same to the Mathieu equation and the geometric relation can be obtained, as mentioned above. And, the pseudo-potential of CIT is the same form to that of Paul trap. Even if η is not constant, the expression is the perfectly same to the expression for constant η. The pseudo-potentials of CIT in Fig. 4 represents that the shape of pseudo-potentials of CIT is almost the same to that of Paul trap. The pseudo-potentials of the CIT show the potential well as like harmonic oscillator near the center of the CIT. However, the potential shape has some different slope compared with that of harmonic oscillator when an ion is located at far from the center of CIT. It means that η is not a constant when the position of ion is getting far from the center of CIT. Therefore, the value of trap parameter varies with the ion's distance from the center of CIT. Also, the change of trap parameter induces the variation of ion's stability. Therefore, the ion's stability depends on ion's position in CIT, which is the big difference from Paul trap. Also, this dependence generates the spatial region for ion stability, we called stability space, in CIT. The rigorous calculation using Eq. (6) indicated also the existence of stability space as shown in Fig. 5.

5. Stability space

Fig. 5 shows a quarter area of stability space calculated by Eqs. (3) and (4) as the functions of μ. The distance

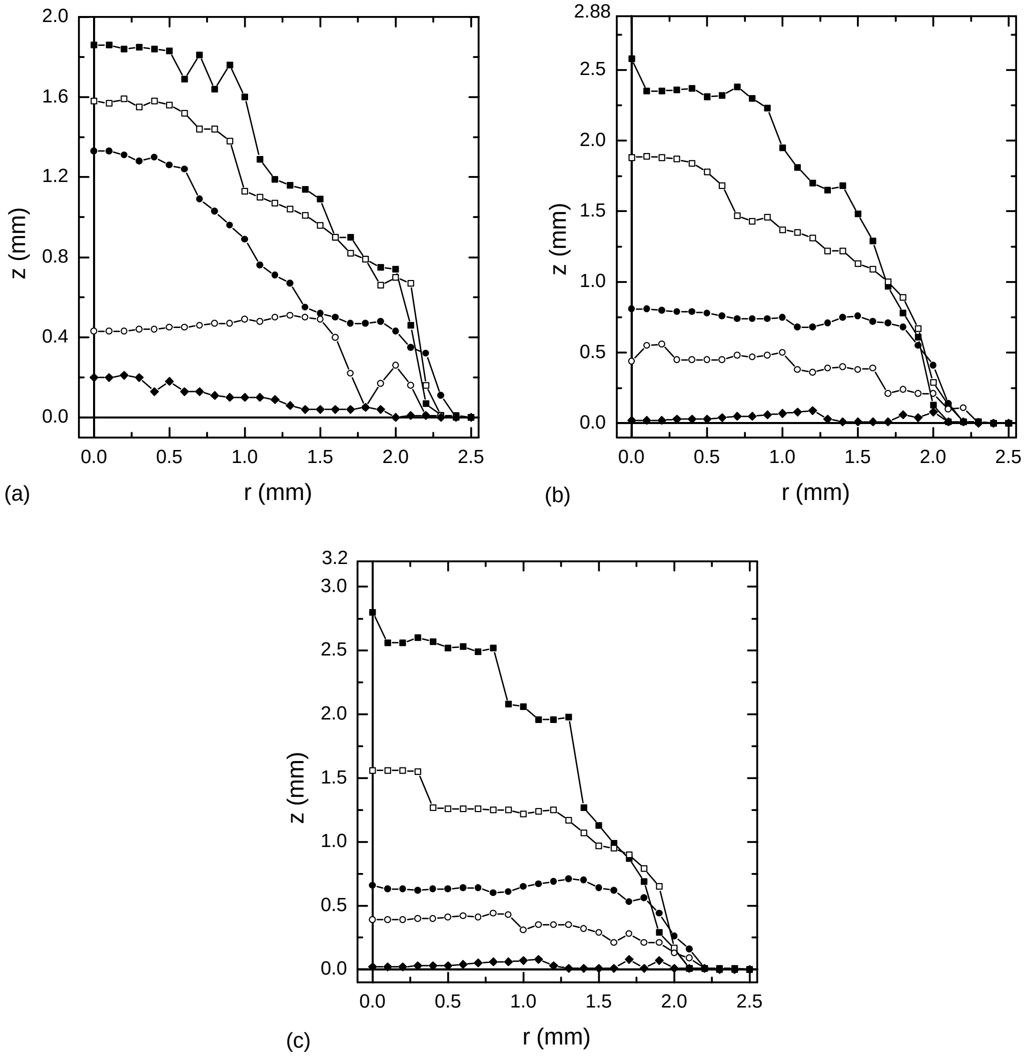

Fig. 5. The stability spaces. The r_1 was fixed 2.5 mm, and the z_1 was fixed at 2.00, 2.88 and 3.2 mm for (a), (b) and (c), respectively. The $q_{z,\mathrm{CIT}}$ was 0.1, 0.3, 0.5, 0.7 and 0.9 for square, hollow square, circle, hollow circle and diamonds. In (b) and (c), the minimum stability space value was lower than 1 μm.

between the center of the CIT and the ring electrode, r_1, was fixed at 2.5 mm and μ were 1.25, 0.868 and 0.781, respectively. When a rf voltage applied to the ring electrode increased, the stability space for *z*-direction decreased. In spite of decreasing the stability space for the *z*-direction, the stability space for *r*-direction was not decreased. This behavior agreed well with the results by Belian and Audoin [12] using Bessel functions and hyper triangular functions. Specially, the size of stability space for the *z*-direction was very small at high q_z. In the Paul trap, an ion is stable up to an ejection rf voltage according to $q_z = 0.908$. Only when a rf voltage reaches the ejection voltage, an ion becomes unstable and the ion ejects from the Paul trap. Our results indicated that an ion in the CIT became unstable before a rf voltage reached the ejection voltage. When the mass selective instability scan method is used to mass spectrometer constitute of the CIT, this result shows that ions in the CIT are ejected before a rf voltage reaches ejection voltage corresponding to $q_{z,\mathrm{CIT}} = 0.908$. This effect should cause a poor resolution of mass spectrum of CIT compared with that of commercial ion trap [20–23]. Therefore, the poorer resolution of CIT than that of commercial ion trap is an intrinsic characteristic.

6. Conclusion

The ion stability in cylindrical ion trap was investigated. At first, the equation of motion in CIT was derived by the modified Bessel function and triangular function. The equations of motion for *r*- and *z*-directions could not be solved analytically since these are complicate coupled each other. The 4th Runge–Kutta method was adopted to calculate numerically the stability region in CIT. The stability region of CIT was very similar to that of Paul trap. The simple geometric relation between Paul trap and CIT ($r_0 = z_1\sqrt{2/\pi\mathbf{A}}$) was suggested, which makes consider the CIT as Paul trap in the case of $\mu < 1.1$. Thus, the ion motion in CIT could be easily expected as like that in Paul trap. Also, this relation supports the reason why previous reported geometries of CIT were near $\mu \approx 0.9$. The pseudo-potential approach provides that the pseudo-potential of CIT had a similar shape of that of Paul trap. The dependence of ion stability on the ion position in CIT, the stability space, was calculated by solving the equation of ion motion, and degradation of the resolution of mass spectrum might be an inherent characteristics of CIT due to the stability space.

Acknowledgements

This research was supported by Korea Dual Use Technology Project (project number: 01-DU-EB-01). Dr. C.H. Oh wishes to acknowledge partial funding from the KOSEF through the Quantum Photonic Science Research Center at Hanyang University. Dr. P.S. Kim wishes to acknowledge the financial support of Hanyang University, Korea, given in the program year of 2001.

References

[1] W. Paul, H. Steinwedel, Z. Naturforsch. A 8 (1953) 448.

[2] R.E. March, J.F.J. Todd, Practical Aspects of Ion Trap Mass Spectrometry, CRC Press, New York, 1995.

[3] R. March, J. Mass Spectrom. 32 (1997) 263.

[4] D.J. Wineland, W.M. Itano, J.C. Bergquist, Opt. Lett. 12 (1987) 389.

[5] W.M. Itano, J.C. Bergquist, R.G. Hulet, D.J. Windeland, Phys. Rev. Lett. 59 (1987) 2732.

[6] W.M. Itano, D.J. Heinzen, J.J. Bollinger, D.J. Wineland, Phys. Rev. A. 41 (1990) 2295.

[7] J. von Zanther, J. Abel, Th. Becker, M. Fries, E. Peik, H. Walther, R. Holzwarth, J. Reichert, Th. Udem, T.W. Hansch, A.Yu. Nevsky, M.N. Skvortsov, S.N. Bagayev, Opt. Commun. 166 (1999) 57.

[8] R.J. Rafac, B.C. Young, J.A. Beall, W.M. Itano, D.J. Wineland, J.C. Berquist, Phys. Rev. Lett. 85 (2000) 2462.

[9] D. Kielpinski, V. Meyer, M.A. Rowe, C.A. Sackett, W.M. Itano, C. Monroe, D.J. Wineland, Science 291 (2001) 1013.

[10] A. Steane, C.F. Roos, D. Stevens, A. Mundt, D. Leibfried, F. Schmidt-Kaler, R. Blatt, Phys. Rev. A 62 (2000) 042305.

[11] E.C. Beaty, J. Appl. Phys. 61 (1987) 2118.

[12] M.N. Benilan, C. Audoin, Int. J. Mass Spectrom. Ion Phys. 11 (1973) 421.

[13] R.F. Bonner, J.E. Fulford, R.E. March, G.F. Hamilton, Int. J. Mass Spectrom. Ion Phys. 24 (1977) 255.

[14] R.E. Mather, R.M. Waldren, J.F.J. Todd, R.E. March, Int. J. Mass Spectrom. Ion Phys. 33 (1980) 201.

[15] J.M. Wells, E.R. Badman, R.G. Cooks, Anal. Chem. 70 (1998) 438.

[16] E.R. Badman, R.G. Cooks, Anal. Chem. 72 (2000) 5079.

[17] O. Kornienko, P.T.A. Reilly, W.B. Whitten, J.M. Ramsey, Rev. Sci. Instrum. 70 (1999) 3907.

[18] O. Kornienko, P.T.A. Reilly, W.B. Whitten, J.M. Ramsey, Rapid Commun. Mass Spectrom. 13 (1999) 50.

[19] H.G. Dehmelt, Adv. At. Mol. Phys. 3 (1967) 53.

[20] G.E. Patterson, A.J. Guymon, L.S. Riter, M. Everly, J. Griep-Raming, B.C. Laughin, Z. Ouyang, R.G. Cooks, Anal. Chem. 74 (2002) 6145.

[21] L.S. Riter, Y. Peng, R.J. Noll, G.E. Patterson, T. Aggerholm, R.G. Cooks, Anal. Chem. 74 (2002) 6154.

[22] J.C. Schwartz, J.E.P. Syka, I. Jardine, J. Am. Soc. Mass Spectrom. 2 (1991) 198.

[23] J.D. Williams, K.A. Cox, R.G. Cooks, R.E. Kaiser Jr., J.C. Schwartz, Rapid Commun. Mass Spectrom. 5 (1991) 327.